Palaeomagnetic and synchrotron analysis of >1.95 Ma fossil-bearing palaeokarst at Haasgat, South Africa

AUTHORS:
Andy I.R. Herries[1]
Peter Kappen[2,3]
Anthony D.T. Kegley[4]
David Patterson[3]
Daryl L. Howard[3]
Martin D. de Jonge[3]
Stephany Potze[5]
Justin W. Adams[6]

AFFILIATIONS:
[1]Australian Archaeomagnetism Laboratory, Archaeology, Environment and Community Planning, La Trobe University, Melbourne, Australia
[2]Physics, La Trobe University, Melbourne, Australia
[3]Australian Synchrotron, X-ray Fluorescence Microprobe Beamline, Melbourne, Australia
[4]Biomedical Sciences, Grand Valley State University, Allendale, MI, USA
[5]Plio-Pleistocene Palaeontology Section, Ditsong National Museum of Natural History, Pretoria, South Africa
[6]Anatomy and Developmental Biology, Monash University, Melbourne, Australia

CORRESPONDENCE TO:
Andy Herries

EMAIL:
a.herries@latrobe.edu.au

POSTAL ADDRESS:
Archaeology, Environment and Community Planning, La Trobe University, Martin Building, Melbourne Campus, Bundoora, Melbourne 3086, Victoria, Australia

DATES:
Received: 11 Apr. 2013
Revised: 17 Aug. 2013
Accepted: 09 Sep. 2013

KEYWORDS:
biochronology; X-ray flourescence; synchrotron radiation; iron; primate fossils; magnetostratigraphy

Palaeomagnetic analysis indicates that Haasgat, a fossil-bearing palaeocave in the Gauteng Province of South Africa, is dominated by reversed magnetic polarity in its oldest, deepest layers and normal polarity in the younger layers. The presence of in-situ *Equus* specimens suggests an age of less than ~2.3 Ma, while morphological analysis of faunal specimens from the ex-situ assemblage suggests an age greater than 1.8 Ma. Given this faunal age constraint, the older reversed polarity sections most likely date to the beginning of the Matuyama Chron (2.58–1.95 Ma), while the younger normal polarity deposits likely date to the very beginning of the Olduvai Sub-Chron (1.95–1.78 Ma). The occurrence of a magnetic reversal from reversed to normal polarity recorded in the sequence indicates the deposits of the Bridge Section date to ~1.95 Ma. All the in-situ fossil deposits that have been noted are older than the 1.95 Ma reversal, but younger than 2.3 Ma. Haasgat therefore dates to an interesting time period in South African human evolution that saw the last occurrence of two australopith species at ~2.05–2.02 Ma (Sts5 *Australopithecus africanus* from Sterkfontein Member 4) to ~1.98 Ma (*Australopithecus sediba* from Malapa) and the first occurrence of early *Homo* (Sk847), *Paranthropus* and the Oldowan within Swartkrans Member 1 between ~2.0 Ma and ~1.8 Ma.

Introduction

The exposed Malmani dolomite to the west of Johannesburg and Pretoria in South Africa is the host rock for thousands of cave systems that have been forming throughout most of the Quaternary (last 2.6 Ma) and perhaps as early as the beginning of the Pliocene (5.3 Ma). These cave systems are well known for their wealth of archaeological and fossil-bearing infills, including abundant hominin remains.[1-3] While a large body of research exists on the hominin-bearing palaeocave deposits such as Sterkfontein[4-6] and Swartkrans[7], recent results from less intensively worked or new fossil localities, such as Malapa[8-11], the Bolt's Farm complex[12,13], Gondolin[1,14-16] and Hoogland[17], have highlighted the importance of wider regional sampling for understanding geographical and temporal variability in Plio-Pleistocene karst development, faunal evolution, taphonomy and palaeoecology that underlie interpretations of the South African hominin and primate fossil record.

Unfortunately, an historical inability to reliably date these fossil localities has limited attempts to integrate the data from South African palaeocaves, as well as to compare the data to the record from eastern African Plio-Pleistocene sites. Some of the earliest attempts at dating the Swartkrans and Makapansgat Limeworks hominin-bearing cave deposits using palaeomagnetism[18,19] produced results, but inappropriate sampling (e.g. drill cores, breccia) as well as mistakes in understanding the stratigraphy of these complicated sites, provided little clarity. Recent improvements in palaeomagnetic correlation methods for South African karstic systems[6,9,10,15,17,20,21] and integration of uranium-lead dating[5,9,10] with electron spin resonance[1,6] have begun to unravel the complex history of these sites; for some deposits, the application of multiple methods has provided the first reliable age estimates[1-3].

The Haasgat cave system is a little explored fossil-bearing palaeocave that lies in the Monte Christo Formation of the Malmani dolomites that forms part of the Schurveberg Mountain Range west of Pretoria, ~20 km northeast of the well-described early Pleistocene karst systems of Sterkfontein, Swartkrans and Kromdraai (Figure 1). Haasgat is located on the Leeuwenkloof 480 JQ farm, positioned between the Gondolin hominin-bearing palaeocave (~4 km to the northeast)[1,14-16] and the Malapa and Gladysvale australopith-bearing palaeocaves (~5–7 km to the southwest).[8-11,21] Limited geological investigation and ex-situ palaeontological sampling in the late 1980s produced a relatively large and diverse sample of extinct baboon, colobus monkey and ungulate species.[22-26] In 2010, geological and palaeontological research was renewed at Haasgat with the aim of more reliably determining the age of the deposit, conducting new excavations of the first in-situ deposits, and undertaking a thorough reanalysis of the previously recovered Haasgat HGD fossil sample.[22] Here we present the first magnetobiostratigraphic analysis of the Haasgat fossil locality.

HOW TO CITE:
Herries AIR, Kappen P, Kegley ADT, Patterson D, Howard DL, De Jonge MD, et al. Palaeomagnetic and synchrotron analysis of >1.95 Ma fossil-bearing palaeokarst at Haasgat, South Africa. S Afr J Sci. 2014;110(3/4), Art. #2013-0102, 12 pages. http://dx.doi.org/10.1590/sajs.2014/20130102

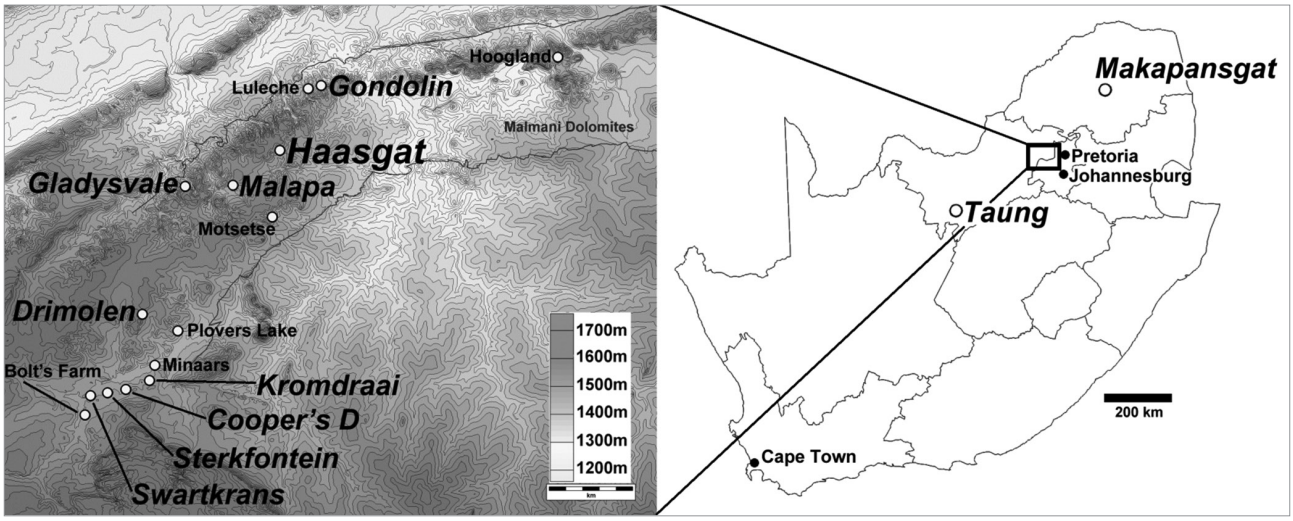

Figure 1: The location of Haasgat within the Cradle of Humankind World Heritage site and its relation to other fossil sites mentioned in the text. Sites with larger font are hominin-bearing sites (except Haasgat) and those with smaller font are vertebrate fossil sites.

History of work at the site, geology and biochronology

Palaeontological deposits in the Haasgat karstic system were first noted in 1987 and led to initial geological description[23] and faunal analysis[24-26] of fossils processed from the extensive ex-situ miner's rubble at the site. Lime mining during the early 20th century removed a large portion of flowstone, stalagmites and stalactites that formed over a basal collapse and left extensive fossiliferous bands of calcified sediments on the walls and ceiling of the mine. In removing these, the miners broke through a wall of speleothem at the end of the fossil tunnel and into the bottom of a more recent shaft that is choked a short distance into another small cave at the surface. The site is unusual compared with many of the fossil-bearing palaeocaves in the region in that the current deposit retains the original structure (roof, walls and floor) of the palaeocave, consisting of a long tunnel that was completely filled to the roof with breccia, conglomerate and fine-grained laminated sediments and speleothem. During the early palaeontological work an unknown quantity of ex-situ breccia from the associated dumpsite was collected and processed, yielding a diverse faunal sample (HGD assemblage) that includes the largest and most demographically diverse accumulations of two primate taxa (*Papio angusticeps* and *Cercopithecoides haasgati*) from a single locality in South Africa.[23-28]

Early publications on Haasgat[23,24] suggested that the elevation of the system relative to the modern valley floor, the erosional deroofing prior to mining and the occurrence of the extinct primate *Parapapio broomi* might indicate a terminal Pliocene age for primary fossil deposition (then about 1.8 Ma). Later the entire papionin sample was reclassified to *Papio angusticeps*[25] and, given the shared occurrence of the species, the age estimate for the site was considered to be contemporaneous with Kromdraai A/B and Cooper's. Kromdraai B is now dated to between 1.8 Ma and ~1.6 Ma[1,2,27], while Cooper's D is dated to between 1.6 Ma and <1.4 Ma[29]. However, no dates exist for the original Cooper's Cave sites on which this correlation was based or for Kromdraai A. Subsequently, Plug and Keyser[26] described an essentially modern ungulate sample and suggested that the deposits maximally formed between 1.5 Ma and 0.5 Ma.

Our work with the HGD assemblage since 2010 has revealed that prior publications considered only a subset (1475 of 2413) of the originally processed ex-situ specimens. Incorporation of the previously undocumented specimens into the HGD assemblage and morphological analysis of the HGD fossils have significantly altered both the faunal list and the biostratigraphic implications of the ex-situ sample.[22] Adams[22] concluded from the data that the ex situ faunal sample likely dated to sometime between ~2.3 Ma and ~1.9 Ma. Given new dates for the first occurrence of the genus *Equus* in Africa in the Omo Shungura lower Member G deposits,[30] the recovery of two species of *Equus* (*Equus capensis* and *Equus* cf. *quagga* [*sensu*[30]]) in the HGD ex-situ sample[22] indicates at least some of the faunal assemblage is younger than 2.31 Ma. (Tuff G is now dated to 2.27±0.04 Ma and the *Equus* fossils are in deposits G1 that are younger than this age, but older than 2.19±0.04 Ma – the age for Tuff G3.[31]) Although neither of the suid craniodental remains were specifically diagnostic, they express crown morphology more advanced than *Metridiochoerus* from Makapansgat Limeworks Member 3 (2.85–2.58 Ma[3,32,33]) but are more primitive relative to *Metridiochoerus* and *Phacochoerus* specimens recovered from later Pleistocene deposits like Cornelia-Uitzoek (1.07–0.99 Ma)[22,34] and overall resemble *Metridiochoerus andrewsi* specimens from Gondolin GD 2 (1.95 Ma to ~1.78 Ma[1,14,15,35]) and *M. andrewsi* and *Phacochoerus* specimens from Swartkrans Member 1 (dating to sometime between 2.25 Ma and 1.80 Ma[7], but most likely <1.96 Ma[1]). The most common bovid species in the HGD assemblage is klipspringer (*Oreotragus* sp.; 38.0% of the bovid assemblage and 15.6% of the total assemblage), which exhibits greater affinity to the sample of the genus from the Makapansgat Limeworks Member 3 deposits (2.85–2.58 Ma) than to that from Gondolin GD 2 (1.95 Ma to ~1.78 Ma[14,15,35]), despite the geographic proximity of Gondolin to Haasgat.[22] As noted above *P. angusticeps* (24.0% of the total Haasgat HGD assemblage) appears to represent an early Pleistocene papionin, although the first and last appearance dates of the species is unknown.[27] And, finally, within the colobine sample (11.0% of the total assemblage), some of the craniodental specimens attributed to the new species *Cercopithecoides haasgati*[28], but recently revised as representing *Cercopithecoides williamsi*[22,36], show some morphological similarities to specimens from Sterkfontein Member 4 (e.g. SWP 495 partial skull and SWP 1735 mandible; 2.6–2.0 Ma[3,5,6]). Collectively, these taxa represent nearly 50% of the identifiable HGD specimens and suggest an age between 2.3 Ma and 1.8 Ma for some of the ex-situ faunas; this time range is useful for magnetostratigraphic analysis because of the occurrence of a number of geomagnetic field reversals and events that have been documented at other South African palaeocave sites (Olduvai event, 1.95–1.78 Ma; pre-Olduvai event, ~1.98 Ma; Huckleberry Ridge event, ~2.04 Ma; and Réunion event, ~2.16 Ma[3,6,9,10,14]).

Detailed site description and sampling

The geology of the site has been described previously[23] and its features, plan and long section are shown in Figures 2–4. The original Haasgat cave appears to have been a long horizontal passage, likely once connected to palaeokarst remnants that occur at the same level along the margins on both sides of the steep valley in which the cave is located. This likely connection indicates that the entire north–south valley itself was once occupied by a now collapsed Pliocene (or earlier) cave system, of which Haasgat was simply one extension. A similar situation

has been envisaged in the mountainous karst at Makapansgat.[37-39] The sediment infilling the main Haasgat passage today is not related to this earlier phase of the cave's life history but to a later phase of breakdown and decay during which the tunnel was truncated by the collapse of the cave and formation of the valley. This episode of erosion and downcutting would have opened the cave to the surface and begun the deposition of sedimentary deposits and fossils. However, this was not the last phase of karstification of the deposit, as shown by the more recent shaft at the end of the fossil tunnel, as well as the remnants of later, much smaller cave passages that formed through the earlier palaeocave fill. A very limited number of fossils has been noted within the fill of these later tunnels and such features could explain the occurrence of what seem like much younger fossils within the ex-situ assemblage,[22] such as *Damaliscus dorcas* and *Connochaetes gnou* (current first appearance date at Cornelia-Uitzoek: 1.07–0.99 Ma[34]). *D. dorcas* is known from Elandsfontein, although these deposits are themselves undated by radiometric methods and have an age estimate of ~1.1–0.6 Ma based on faunal correlation with South African sites and preliminary palaeomagnetism.[40,41] Moreover, this species has previously been noted at Swartkrans Member 2 (1.7–1.1 Ma[35,42]) and the genus is recorded at several sites post 2 Ma (e.g. Swartkrans Member 1[35]), but the specimens have not been designated to species level. These species are represented by only a handful of fossils (NISP 8[21]) out of the 1446[22] identifiable specimens, at least 50% of which suggest an earlier time period (see above). The site has had only extremely limited secondary karstification (one later and limited phase that is infilled with uncalcified dark brown sediment that is distinct from the red to reddish brown siltstones and mudstones of the older phase), unlike complex multi-generational sites such as Sterkfontein and Swartkrans where serious mixing is likely to have occurred between older and younger Members.[1] As such, we consider the bulk of the ex-situ fauna to come from deposits equivalent to the single phase of karstification being dated in this analysis, especially given that the main bone beds have been identified within the interior, older part of the cave.

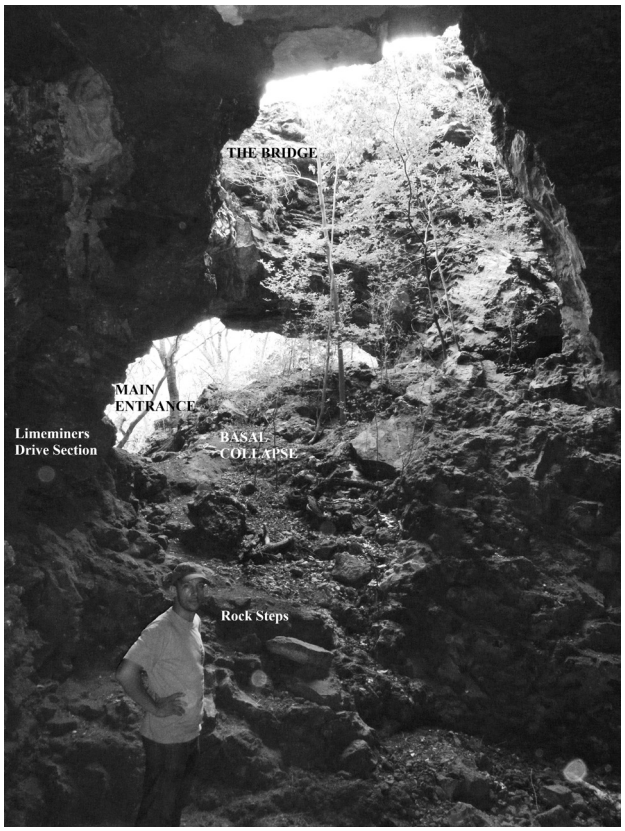

Photo: AIR Herries; Jason Hemingway in front.

Figure 2: Major features of the Eastern Deposits of the Haasgat mine and its palaeocave deposits looking east from the entrance to Tetley's Hall (perspective shown in plan of Figure 4).

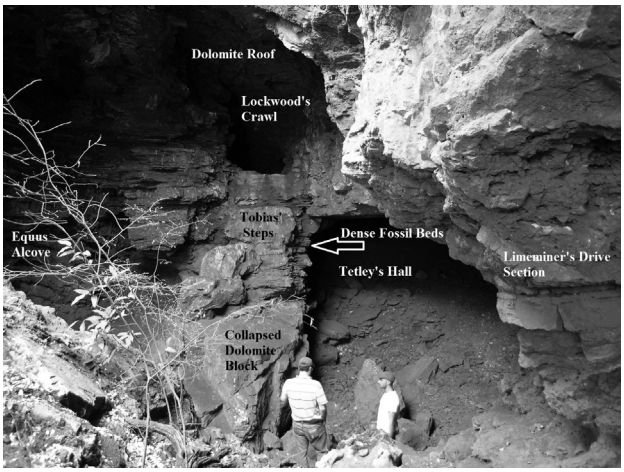

Photo: AIR Herries; Jason Hemingway and Colin Menter can be seen in the photo.

Figure 3: Major features of the Western Deposits of the Haasgat mine and its palaeocave deposits looking west from beneath the Bridge (perspective shown in plan of Figure 4).

Today, Haasgat consists of a large mined tunnel running almost east–west into the hillside with a large entrance at its easterly end. The current cavity is almost entirely the result of lime mining activity for speleothem which has removed a number of generations of cave infill in varying stages of calcification. Unlike many palaeocave fills of this type, in which the original cave has been completely infilled with sediment and partly eroded away, the roof and walls have been preserved in the rear section of the tunnel, while the floor remains buried under both the original basal cave rubble and subsequent mining rubble. The mined tunnel ends at a slope up into the bottom of a high chocked shaft (Partridge Aven) that has been infiltrated by tree roots from vegetation growing in the small cave above the fossil site (Keyser Pot). Before the lime mining there would have been no access horizontally into this part of the system as the current route would have been filled with heavily calcified sediment and speleothem. It appears that Partridge Aven was at some time at least partially filled by sediments as shown by the sediment remnants adhering to its upper reaches of the Aven as viewed from below. How Keyser Pot and Partridge Aven relate to the main palaeokarstic fill is uncertain, but the impression is that it is a much younger fill from a later phase of karstification related to vertical, rather than horizontal, development. The reuse of palaeokarstic conduits by water and the development of new cave passages within old palaeokarst is a common feature of caves in this part of South Africa and can also be seen in other South African dolomite areas such as at the Sudwala Caves (Herries personal observation). This situation is in part related to the fact that calcified palaeokarst contains purer calcite and is thus more easy to dissolve than the dolomite.

A number of morphological features exist in the current cavity (mine) that aid understanding the magnetobiostratigraphic interpretation and they will be briefly described based on a person entering from the main eastern entrance to the mine (Figures 2–4). At the entrance to the mine is a large platform of rubble from lime mining operations into the Haasgat palaeocave deposits. This mining talus cone, which extends some 30 m down the hillside to the valley floor, appears to have served as the source for at least some of the 1988 HGD ex-situ fossil sample. Palaeocave fill outcrops directly onto the hillside, and prior to mining the outline of the fossil tunnel would have been visible after vegetation was cleared. It is evident that the lime miners began by creating an east–west drive through the palaeocave fill and along the very northern wall of the tunnel. This drive also cut into the heavily calcified basal dolomite and chert collapse rubble (basal breccia) that formed as the tunnel developed as a result of the roof collapse. Despite subsequent mining, the outline of this drive is still preserved. The drive seems to have stopped at the approximate position of what is now a buttress of palaeocave remnants adhering to the north wall of the cave and has been termed the 'Limeminer's Drive Section' (LDS). This buttress consists of a series of

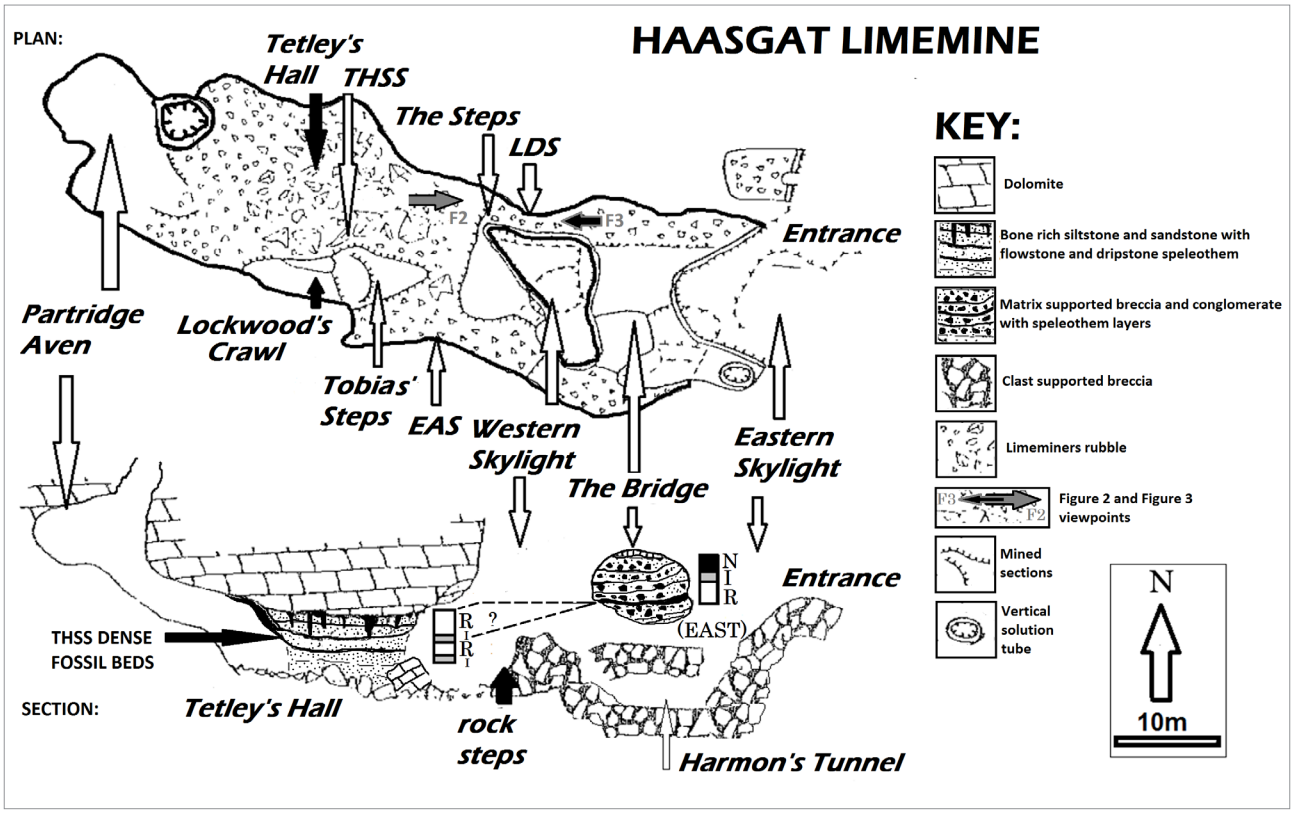

THSS, Tetley's Hall Southern Section; LDS, Limeminer's Drive Section; EAS, Equus Alcove Section

Polarity: N, normal; I, Intermediate; R, reversed

Figure 4: A plan view and a cross-sectional view of the Haasgat Limemine (redrawn using data of Keyser and Martini[22]) showing the major features and stratigraphy described in the text and composite palaeomagnetic polarity of the western and eastern sections. The location of the main in-situ bone bed is shown, as are the perspectives of Figures 2 and 3.

interstratified speleothem and sandstone at its base, grading up into finer grained siltstone that connects with sediments outcropping in the roof at the rear of the cavity. As a result of its isolation, the sediments in this buttress were not sampled in this initial study.

The Limeminer's Drive also passes under a large bridge of palaeosediment fill (the Bridge Section East/West; BSE/BSW) that is connected to both the northern and southern walls of the tunnel (Figures 2 and 3). A small remnant of the original tunnel roof is preserved at the very top of this Bridge and sampling from this roof to the base of the sediments was undertaken on both its east and west face using single rope technique.[40] This sequence consists mostly of conglomerate and breccia deposits that show that this part of the palaeosediments was closer to the entrance than those in the western sector of the tunnel. It also indicates significant waterflow through this part of the cave which would have been responsible for winnowing fine-grained material into the deeper western sections of the tunnel, which is dominated by fine-grained and well-laminated siltstone, sandstones and mudstones. Because of the more brecciated nature of the sediments in the Bridge Sections, sampling for suitable palaeomagnetic samples was more difficult, as breccia rarely records good palaeomagnetic signals. Breccia's poor signal is because it forms as a result of rapid collapse, and so the magnetic grains have no mechanism for accurate orientation and fossilisation of the field direction at the time of deposition. Moreover, the large number of inclusions in breccia causes a randomisation of the magnetic signal because each clast has its own independent magnetic polarity and direction. Fortunately, some finer-grained siltstone layers do occur throughout the sequence, as do flowstone layers, and these layers were the main target for palaeomagnetic analysis.

At its base the Bridge sequence rests on a large fallen dolomite block that sits on the top, but partly within the basal breccia that was excavated around by the limeminers. Beneath this fallen block on the eastern side of the bridge a hole leads down into a lower passage that, at least in part, has been formed through the original basal collapse breccia of the palaeocave (Harmon's Tunnel) by later karstic processes than those that formed and infilled the palaeocave. The deposits exposed in this tunnel are apparently sterile breccias and no sampling was undertaken in this study. This tunnel leads through and back up to '*Equus* Alcove' and into the tunnel's eastern section (see below). On either side of the Bridge there are two large skylights (Eastern and Western Skylights) to the surface that are the product of later opencast mining from the surface. The Western Skylight ends at the beginning of 'Tetley's Hall', the largest entirely subterranean portion of the current cavity and the point at which the original roof of the tunnel is entirely preserved. Beneath the Eastern Skylight the floor consists of two large collapsed dolomite boulders and it is at roughly this position that the Limeminer's Drive ends at a series of artificially formed rock steps that lead down to the rubble-filled modern floor of the mine.

Climbing up a slight slope from the modern floor to the left (south) from these steps brings you to a long alcove along the southern wall of the tunnel which preserves a varying thickness of fine-grained, well-laminated palaeocave fill with very thin (a few centimetres at most) interstratified flowstones. This area has been termed the '*Equus* Alcove Section' (EAS) because of an exposed in-situ *Equus* metacarpal calcified within these deposits. At the eastern end of this alcove are a series of massive mined steps of fine-grained calcified sediment (Tobias' Steps) that can be climbed into a higher tunnel near the cave roof (Lockwood's Crawl). The walls of Lockwood's Crawl consist of very finely laminated

mudstone with the occasional thin flowstone layers (a few centimetres thick) and, near the exposed dolomite roof, quite dense layers of fossils. The original dolomite roof of the cave is exposed here and shows clear signs of anastomosis (the development of a network of branching, intersecting and rejoining tubes). Cave anastomoses are generally formed by dissolution of the dolomite by slow, poorly directed, phreatic flow along a bedding plane (here forming a westerly sloping roof) in shallow dipping rock. Such features represent an important process in the early stages of cave development and are a primary driver of roof collapse and the slow vertical development of cave passages that are primarily developing in the horizontal plane as a result of major bedding control and insoluble chert layering.

The sediments making up Tobias' Steps were sampled for palaeomagnetic analysis and during sampling a number of primate fossils were recovered. In an alcove at the base of these steps a complete primate mandible was also present, indicating that larger, more complete fossils occur in the fine-grained silts that could not have been washed there by winnowing processes from the entrance breccia. Tobias' Steps form the beginning of the southern wall of Tetley's Hall and the eastern end of Tetley's Hall Southern Section (THSS) and it is here that the oldest and thickest fossil-bearing sediments in the Haasgat depositional sequence are exposed. This section was also sampled for palaeomagnetic analysis; it consists of a series of fine-grained siltstone and sandstones regularly interstratified with thin flowstones and sporadically interstratified with thicker flowstones up to 0.12 m deep. The source for these flowstones is a series of smaller stalagmites and one large stalagmite boss which formed at the rear of the tunnel and is in part what separated Partridge Aven from the palaeocave sediments. The deposits at the eastern and western ends of THSS and in Tobias' Steps are well calcified, while deposits in the middle of THSS are partly decalcified, which is likely a result of the formation of a later cavity through the palaeocave fill in this area that has been mined away. The northern wall of Tetley's Hall consists almost entirely of the dolomite and chert wall of the ancient tunnel covered by a wad in places (e.g. manganese dioxide residue from the erosion of the dolomite prior to the opening up of the cave to the surface). Following the southern wall of Tetley's Hall leads to a point where the far end of Lockwood's Crawl punches through the palaeocave fill about 2.5 m above the current floor and enters what is almost the furthest point of Tetley's Hall. Beyond this point the original cave was filled with speleothem that was mined through and now forms a slope up into the base of Partridge Aven. The current floor of Tetley's Hall is made up of limeminer rubble, and palaeocave sediments can be seen disappearing beneath this rubble on the southern wall of Tetley's Hall (THSS).

The roof of Tetley's Hall is composed of sediment that also outcrops within Lockwood's Crawl (Lockwood's Crawl Section) and which can also be seen on the edge of the Western Skylight. Within the Skylight a series of flowstone layers and speleothems can be seen to have been deposited on the basal deposits that are equivalent to those in THSS and have been infilled around and capped by later sediment that outcrops both in Lockwood's Crawl and in the top of the EAS. As such there is contiguous stratigraphy between the basal deposits in Tetley's Hall (THSS) through the sediments outcropping in Lockwood's Crawl (LCS) and EAS and up into the youngest deposits exposed in the top of the Bridge Sections (BSE/BSW). However, in some cases it is difficult to estimate the exact layers that correlate because of remnants of unmined speleothem adhering to the walls and obscuring parts of the sections. Despite this, as you progress deeper into the cave from the entrance the deposits exposed in the walls generally get older, with the base of the Bridge Sections contemporary with the upper part of the LCS, EAS and THSS. These are more informally referred to as the Eastern (BSE/BSW, LDS) and Western Deposits (LCS, EAS, THSS). The relationship between the deposits in the LDS and the Western Deposits is more difficult to determine but generally the LDS deposits are older than the deposits in the Bridge Section and as such may be partly contemporaneous with the base of the Western Deposits. Work on the geology is ongoing using detailed stratigraphic mapping and micromorphological analysis that will help tie the various sections and layers together to create an accurate composite stratigraphy.

Palaeomagnetic methodology

Palaeomagnetic sampling was exclusively undertaken by block sampling with a hammer and chisel using the single rope technique for safety.[43] Because the cave environment is dark, the samples were oriented before removal with a region 4 Suunto cave surveying compass and clinometer. Work was undertaken at the Australian Archaeomagnetism Laboratory (TAAL) at La Trobe University (TAAL: www.archaeomagnetism.com) and the University of Liverpool Geomagnetism Laboratory (ULGL) with the magnetic cleaning of samples undertaken on the same equipment at both laboratories as part of an inter-laboratory comparison. The declination of the final results were then corrected to account for local secular variation using the 11th-generation International Geomagnetic Reference Field model through the British Geological Survey[44] (-14.859° declination and -55.828° inclination). Sub-samples from each layer or block were subjected to a range of magnetic demagnetisation techniques in order to isolate the characteristic remanent magnetisation (ChRM) from more recent viscous overprints. A series of sub-samples from each block or layer were subjected to a 11–17 point alternating field demagnetisation using a Molspin© (UK) or ULGL in-house-built alternating field demagnetiser, thermal demagnetisation using a Magnetic Measurements© (UK) MMTD80a and hybrid demagnetisation consisting of a series of initial alternating field demagnetisation cleaning steps between 8 and 12 millitesla (mT) followed by thermal demagnetisation.[6,9,14,20] Samples were measured on an AGICO© (Czech Republic) JR6 magnetometer with a noise of 2.4 μA/m. Sub-sample directions were defined using principal component analysis and were accepted with a median angle of deviation of $<15°$. Final directions for each block or layer were defined using Fisher statistics using the FISH2 program (written in house at ULGL) and normal and reversed polarity was defined based on the palaeopole direction. Samples with palaeolatitudes of $<+45°$ or $<-45°$ were defined as intermediate and those between $+45–60°$ and -45–60° were defined as intermediate normal or reversed, respectively. Those with palaeopoles greater than $+60°$ and $-60°$ were defined as normal or reversed polarity, respectively. Mineral magnetic measurements were undertaken with a Bartington© (UK) MS3 magnetic susceptibility system at TAAL and a Magnetic Measurements© variable field translation balance at ULGL.

X-ray fluorescence microscopy

X-ray fluorescence microscopy (XFM) analyses were performed at the XFM beamline[45] at the Australian Synchrotron in order to investigate elemental distributions across speleothem cross sections. For the measurements, the beam size was set to ca. 5x5 mm^2 using Kirkpatrick-Baez mirrors. The incident photon energy was chosen as 18.5 keV, thus permitting excitation and detection of the trace metals of interest (Fe, Mn, As, Sr and others). Elemental maps were collected by scanning vertically mounted samples through the beam using x-y-translation stages while simultaneously collecting X-ray fluorescence from the sample with the 384-pixel Maia detector.[46] Maps were typically collected over cm^2 areas at a resolution of 5–10 mm, thus resulting in images of several megapixels size (for specific sampling details see corresponding figures).

Results

Mineral magnetic measurements (Figure 5) were undertaken on sister samples throughout the sequence to establish the main remanence carrier and possible effects caused by changes in mineralogy and magnetic grain size. The samples have extremely high magnetic susceptibility (χ_{LF}; up to 5.74 x10^{-6} m^3/kg^{-1}; Table 1) indicating significant proportions of ferromagnetic material, which is also confirmed by the high magnetic intensity of the remanence not only within the sediment samples, but also within the speleothems. The high magnetic susceptibility can be accounted for by the large proportion of fine- to ultra-fine-grained (<0.05 μm) single to superparamagnetic ferrimagnetic material as shown by frequency dependence of magnetic susceptibility (χ_{FD}%) values of between 6.20% and 15.8%, the latter of which is close to the maximum value expected for natural samples.[46] Isothermal remanent magnetisation acquisition curves and hysteresis loops further indicate the low coercivity, ferrimagnetic nature of the samples and Curie points of just less than 600 °C indicate the dominant mineral is magnetite.[48]

The presence of a low temperature tail below -150 °C in the low temperature magnetic susceptibility curves also indicates magnetite over maghaemite. The remanence within the samples is removed between 500 °C and 600 °C, which further confirms that it is primarily carried by magnetite. Low temperature magnetic susceptibility curves indicate no presence of a Verway transition and as such the low coercivity is interpreted to be as a result of viscous single domain grains close to the superparamagnetic boundary, as also indicated by high χ_{FD}%, rather than multi-domain grains. The stability of the samples during heating with little change in χ_{LF} and general reversibility of the thermomagnetic curves further supports this hypothesis, although a slight drop in magnetisation on cooling (Figure 5) in some samples may indicate the presence of maghaemite. A non-saturation of the IRM curves by 100 mT also indicates a proportion of larger stable single domain grains that carry the primary remanence.

X-ray fluorescence microscopy (XFM) studies at the Australian Synchrotron indicate that the majority of iron (Fe) phases occur as discrete horizontal bands within the flowstone (Figure 6) and correlate with higher concentrations of arsenic (Figure 7), which has been suggested to correlate to warmer, more humid phases with increased erosion.[49] This finding is further confirmed by the presence of manganese-bearing structures and their co-location with arsenic (Figure 7), the former of which would have come from greater dissolution of the dolomite host rock.

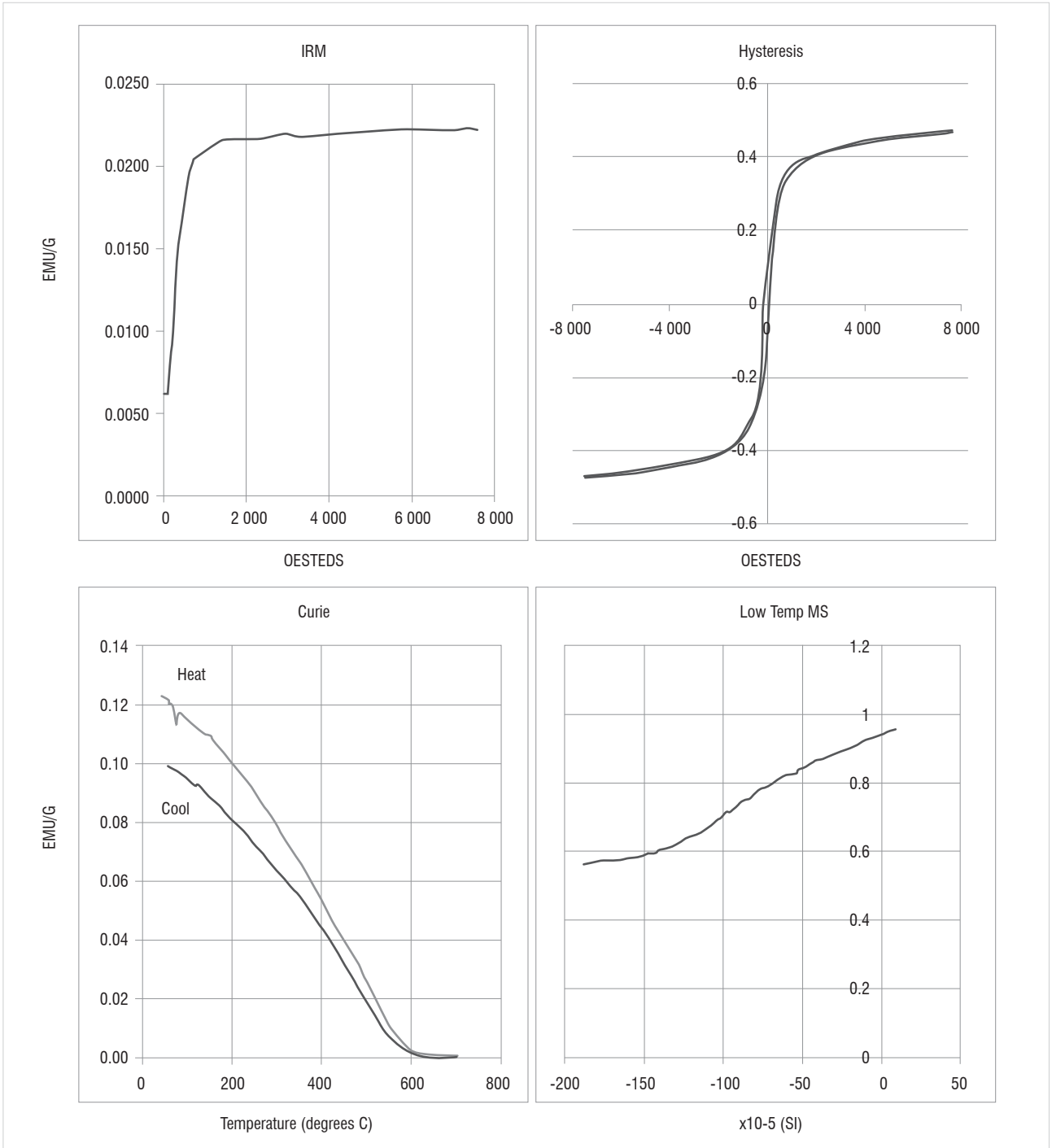

Scale: 2 mm x 2 mm

Figure 5: Mineral magnetic measurements – isothermal remanent magnetisation (IRM), hysteresis, thermomagnetic curve (Curie) and low temperature magnetic susceptibility (MS) – of a siltstone sample from Haasgat.

Table 1: Palaeomagnetic and mineral magnetic results from the Haasgat (HGT) fossil site

Sample	Section	Composite height (m)	χLF	χFD%	Declination	Inclination	Median angle of deviation	Number of samples	K	Palaeolatitude	Polarity	Age (Ma)	Deposit
HGTBWa	BSW	-0.30	2.26	11.62	18.9	-64.3	5.7	3	114	64.6	N	>1.78	Siltstone in breccia
HGTBWTb	BSW	-0.73	2.78	5.79	42.1	-63.7	2.6	3	78	51.0	IN		Siltstone in breccia
HGTBWc	BSW	-1.56	2.66	9.43	20.5	-44.9	5.7	3	205	71.5	N		Siltstone in breccia
HGTBEa	BSE	-2.08	3.44	9.24	329.0	59.1	13.5	3	4	18.5	I	~1.95	Siltstone in breccia
HGTBWd	BSW	-2.43	3.40	7.90	216.2	27.1	10.4	3	24	-54.3	IR		Siltstone in breccia
HGTBEb	BSE	-3.13	4.81	8.58	189.0	38.7	6.7	3	21	-81.0	R		Siltstone in breccia
HGTBWe	BSW	-3.73	1.39	5.32	208.5	52.1	5.3	5	36	-64.2	R		Flowstone
HGTLCa	LCS	-4.37	3.67	9.08	183.3	58.1	5.8	5	361	-76.4	R		Mudstone
HGTLCb	LCS	-4.72	4.67	8.58	176.9	63.7	2.4	3	238	-70.0	R		Mudstone
HGTTHa	THSS	-4.79	0.03	N/A	41.1	21.0	5.1	3	56.5	35.9	I		Flowstone
HGTTHb	THSS	-5.55	3.84	8.58	178.8	61.3	1.5	3	570	-73.0	R	<~2.3	Siltstone
HGTTHc	THSS	-5.90	2.44	7.62	175.8	61.1	4.4	4	30.4	-73.0	R		Siltstone
HGTTHe	THSS	-7.00	3.18	8.47	53.1	30.2	4.3	4	26.2	23.6	I		Siltstone

BSW, Bridge Section West; BSE, Bridge Section East; LCS, Lockwood's Crawl Section; THSS, Tetley's Hall Southern Section; N, normal; I, intermediate; R, reversed.

The XFM data equally shows that Fe-rich layers are strontium (Sr) poor and vice versa (Figure 6). This patterning indicates that the remanence of these bands of Fe is dominated by detrital material that was brought into the cave and deposited over the flowstones and then calcified into their growth structure. However, Fe is also scattered in a vertical pattern in some sections that appear to be related to crystal growth and as such some Fe may have been deposited as detrital material in the drip water or precipitated with the calcite. Weak Fe phases such as goethite can often be found holding a chemical remanence (CRM) within areas of calcite flowstone where no detrital contamination occurs[50,51] and this may be the case here. While such CRMs are generally masked where detrital contamination also occurs within the bands, such CRMs can account for low temperature components in thermal demagnetisation curves,[50-53] as goethite dehydrates to haematite on heating through 150-300 °C.

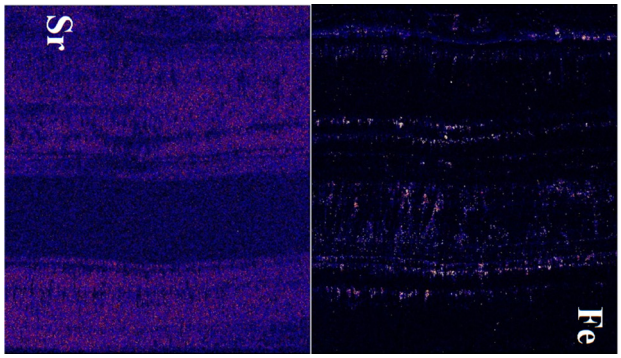

Scale: 1 mm x 6 mm

Figure 6: Synchrotron X-ray fluorescence microscopy data showing the negative correlation between iron (Fe) and strontium (Sr) in a flowstone at Haasgat. The Fe distribution (lighter in the figure) is dominated by the layering of the calcite in the flowstone and is likely detrital from flooding events between flowstone formation. However, it appears that some Fe also occurs along crystal growth boundaries between these laminated layers and may have been introduced into the flowstone during calcite formation. Areas of higher strontium are lighter.

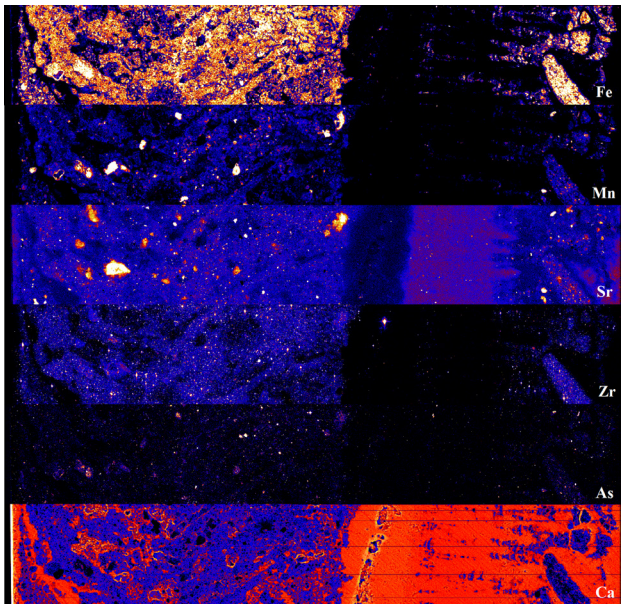

Figure 7: Synchrotron X-ray fluorescence data showing the correlation of iron (Fe) with manganese (Mn) and arsenic (As) versus the structure of the calcite (Ca; calcium) in the flowstone. The high Fe portion on the left of the specimen represents a thick flood layer within the flowstone. In the right-hand side of the specimen, large Fe-rich sediment clasts can be seen occurring within the Ca-rich portion of the flowstone. In the lower section, Fe can also be seen occurring as another thinner layer within the flowstone, as well as along crystal boundaries. (Note: the darker the image the less there is of each element.)

Fe is quite regularly distributed within the Haasgat flowstones (Figure 6) and as such the remanence of standard 25-mm palaeomagnetic cores is measuring the remanence of multiple flood events. In contrast to the calcified sediments which hold a post-depositional remanent magnetisation formed after dewatering and compaction of the sediments, the remanence in speleothem is a true depositional remanent

magnetisation that is formed extremely soon after precipitation over and calcification of the flooding sediment surface, perhaps within a few days or weeks.[50,52,53] There is also some evidence in the XFM data that Fe may have been deposited in the flowstones from precipitation from water as Fe seems to also be dispersed within the calcite crystal growth patterns (Figure 5). This material is likely to be instantaneously locked in and should provide an extremely good record of the ancient field and can often be more reliable than the sediments that surround them because mud cracks, slope effects and other features can cause inclination shallowing or changes in the declination values during post-depositional compaction. The upper flowstone sampled at Haasgat from the Bridge Section records a stable reversed polarity direction (Table 1). However, the flowstone sampled from Tetley's Hall records an intermediate polarity. Based on the XFM data, there is no reason to suggest that this result is because of the recording medium, and it is possible that this result represents a true field deviation and perhaps the edge of a short reversal event or excursion.

The majority of deposits from the site formed during a long period of reversed magnetic polarity (Table 1; Figures 4 and 8). The majority of samples record a stable magnetic polarity with low median angle of deviation values that is both consistent between different sub-samples from the same block (as shown by the low K values) and between samples from different blocks in the same part of the sequence. Reversed samples have declinations of 176–216° and inclinations between +50° and +64°. Normal polarity samples have declinations between 18° and 45° and inclinations of -45° to -69° and so the results show good dipolar dispersal. Some samples do have much shallower mean inclination values (-27° to -45°) that could be a result of post-depositional effects; however, these samples are all on either side of the reversal and they are more likely true field directions related to the polarity reversal. Some individual samples did show inclination shallowing that is more likely related to wetting and drying cycles and fossil mud-cracks are seen within the layers. Directions that are entirely intermediate in nature are also recorded, notably during the reversal from reversed to normal polarity in the Bridge Section, and this definitely represents geomagnetic field change. For a very high proportion of samples (>90%), a stable remanence was recorded (Table 1; Figure 7), which is in part a result of the well-laminated siltstone and flowstone nature of the majority of the deposits and the fact that more brecciated layers, notably in the Bridge, were avoided during sampling. However, the large amount of breccia has led to larger gaps in this part of the sequence. Samples from the Bridge Sections record reversed polarities at the base and normal polarities at the top (Table 1). Samples from the exposures within Lockwood's Crawl (LCS) all record reversed polarity as do sediments containing dense layers of fossils in the top of THSS. Below the fossil layers, the deposits contain a mixture of reversed and intermediate polarities. It is noticeable that well-indurated samples from Tobias' Steps record reversed polarities while those from the same layers exposed in THSS give intermediate polarities. This finding appears to be a result of decalcification and recrystallisation of the calcite within the THSS deposits related to the later phase of passage formation outlined above. In sum, the Haasgat sequence indicates a change from a longer period of reversed polarity in the lower Eastern Deposits, punctuated by periods of intermediate polarity towards its base, to normal polarity in the upper Western Deposits in the Bridge.

Discussion and conclusions

With two species of *Equus* recovered within the ex-situ HGD faunal sample[22], and a nearly complete *Equus* metacarpal exposed in the in-situ calcified sediment sequence at a level equivalent to reversed polarity layers in THSS, the majority of the fossiliferous deposits are likely not older than ~2.3 Ma (the oldest occurrence of *Equus* in Africa[30,31]) and the majority of other fauna suggest the site is older than Gondolin GD2 at 1.95–1.78 Ma[1,22,35]. An age assessment for the deposits based on magnetobiostratigraphy requires the identification of a longer period of reversed polarity as seen in the Western Deposits and the base of the Bridge Deposits followed by a reversal to a period of normal polarity as seen in the top of the Bridge Deposits (Figures 4 and 9). Only one major reversal from reversed to normal polarity occurs within the 2.3–1.8 Ma time period, at the beginning of the Olduvai SubChron at ~1.95 Ma[54,55] (Figure 9). While several short geomagnetic field events also occur in this time period at ~1.98 Ma (Pre-Olduvai), ~2.05–2.02 Ma (Huckleberry Ridge) and ~2.21–2.14 Ma (Réunion), and have been found in other South African palaeocaves,[3,6,10] they almost exclusively occur in speleothem, not cave sediments. The same magnetic reversal has been found in flowstone speleothem in different caves, suggesting that such flowstones could be used as marker beds between sites, akin to the volcanic tuffs of East Africa. As a result of the potential rapid accumulation of sediments, compared to flowstone, the normal polarity period (which covers about 2 m of the total 7 m of section analysed) could represent such short polarity episodes (generally <6 ka in length[54]), but it is much less likely. The chances of the sediments forming during such a short reversal are highly unlikely when compared to the more parsimonious explanation that they were deposited during a longer period (~170 ka) of stable polarity such as the Olduvai SubChron (1.95–1.78 Ma). That being said, such a short period has been suggested to encompass the deposition of the Malapa fossils[10], even though deposition within the Olduvai SubChron was previously considered more likely[9]. The intermediate polarities noted in speleothems towards the base of the sequence (in THSS) are more likely to relate to such short reversal events that were perhaps not entirely recorded or have been missed during the current sampling phase at the site. Given the short lock in time of speleothem and the fact that the XFM data indicate that Fe distribution in the speleothems is within discrete bands, the intermediate polarities (Figure 8c) are considered to be true field directions rather than an effect of the recording medium.

Further detailed sampling will concentrate on increasing the sample resolution in this area of the cave. As such, the Eastern Bridge Deposits at the front of the cave most likley date to either side of 1.95 Ma, although an older age between 2.21 Ma and 1.98 Ma cannot be ruled out at this stage. The fossil rich Western Deposits (EAS, LCS, THSS) at the rear of the cave all date to a period prior to 1.95 Ma. The question that remains is how much older the Western Deposits are than 1.95 Ma, given that the next oldest major reversal is the Gauss–Matuyama boundary at 2.58 Ma. The occurrence of *Equus* would suggest that it is unlikely to be older than ~2.3 Ma, although in-situ *Equus* remains have not been recovered from the base of the sequence deeper than ~5 m. More detailed palaeomagnetic analysis could potentially identify one or more of the small geomagnetic reversals in this time period (~2.16 Ma, ~2.04 Ma, ~1.98 Ma[3,6,10]) but this identification will require extremely detailed sampling of the deposits. Uranium-lead dating of flowstones in the base of the sequence would also help refine the age.

Given the occurrence of the reversal at the beginning of the Olduvai SubChron at ~1.95 Ma (or other reversal between 2.21 Ma and 1.98 Ma), it is also possible that the whole deposit and its fossils may not be much older than this reversal, especially given that it is currently unclear exactly how the Western and Eastern Deposits correlate exactly as the stratigraphy is partly obscured between them. The Western Deposits are certainly older than the reversal identified but they cannot be directly stacked beneath the Eastern Deposits to create a composite stratigraphy as the siltstones of the Western Deposits were in part formed by winnowing of the Eastern breccias and so are partly contemporary. It is possible that flowstone layers towards the base of the Eastern Deposits correlate with the flowstone deposition also noted in the middle of the Western Sequence. If this were the case then the reversed polarity period would go from covering ~5 m of stratigraphy to ~4 m, although this is still double that covered by the normal polarity period. Further detailed sampling and stratigraphic work will hopefully resolve many of these issues but at present a good estimate for the age of the deposit is between 2.3 Ma and 1.8 Ma, perhaps around ~2 Ma.

At an age between 2.3 Ma and 1.8 Ma, Haasgat is potentially pene-contemporaneous with a number of other deposits and fossils in South Africa (Figure 9) including *Australopithecus sediba* at Malapa at ~1.98 Ma[10], the last occurrence of *Australopithecus africanus* (Sts 5; 'Mrs Ples') in Sterkfontein Member 4 at ~2.05–2.02 Ma[3,6] and the first occurrence of early *Homo* (SK 847), *Paranthropus robustus* and the Oldowan tool industry in the Hanging Remnant of Swartkrans Member 1

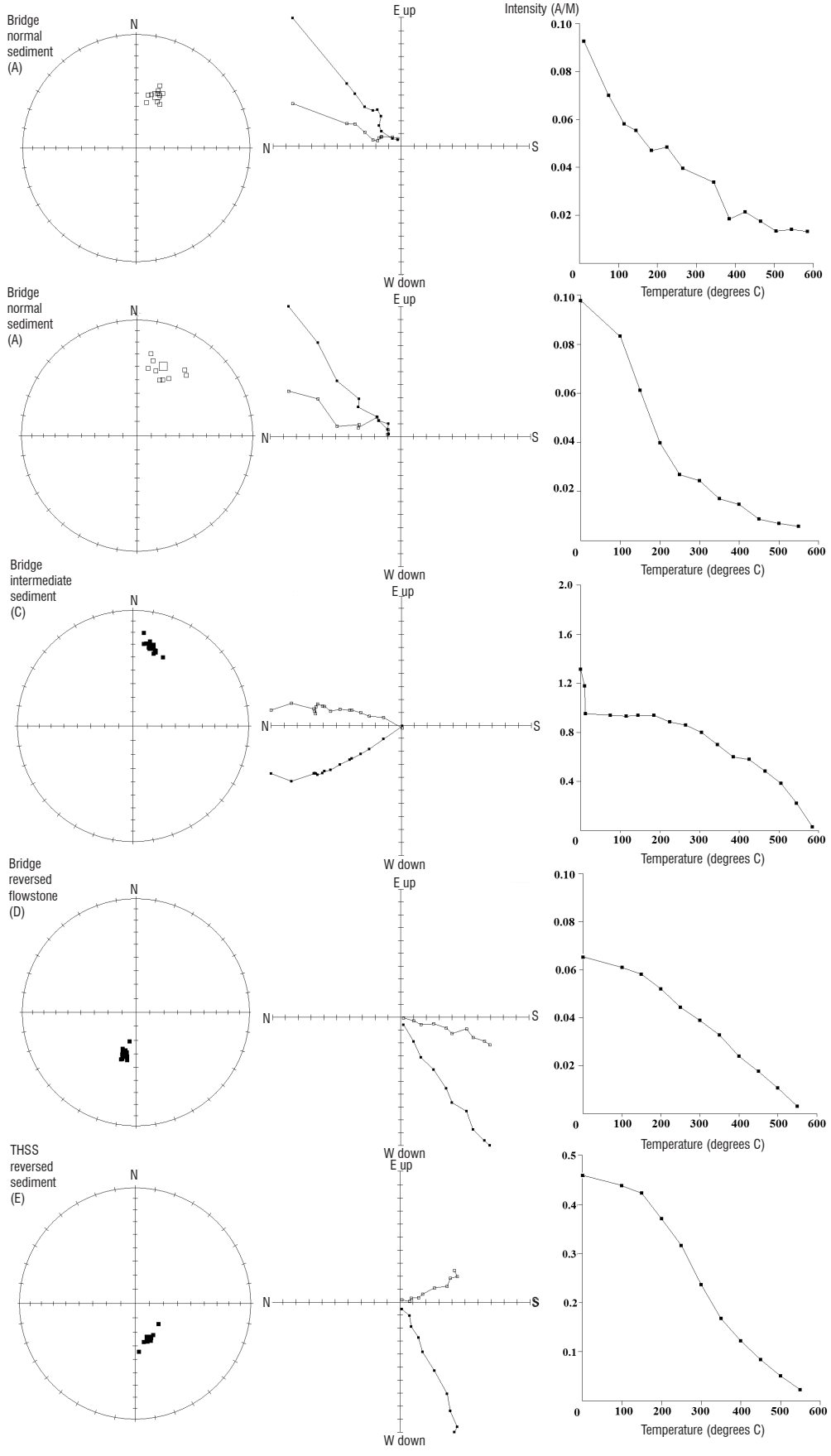

Figure 8: Demagnetisation spectra (stereo, Zijderveld and intensity plots) for representative (a,b) normal, (c) intermediate and (d,e) reversed polarity siltstone within (a–c) breccia, (e) mudstone and (d) flowstone samples from Haasgat.

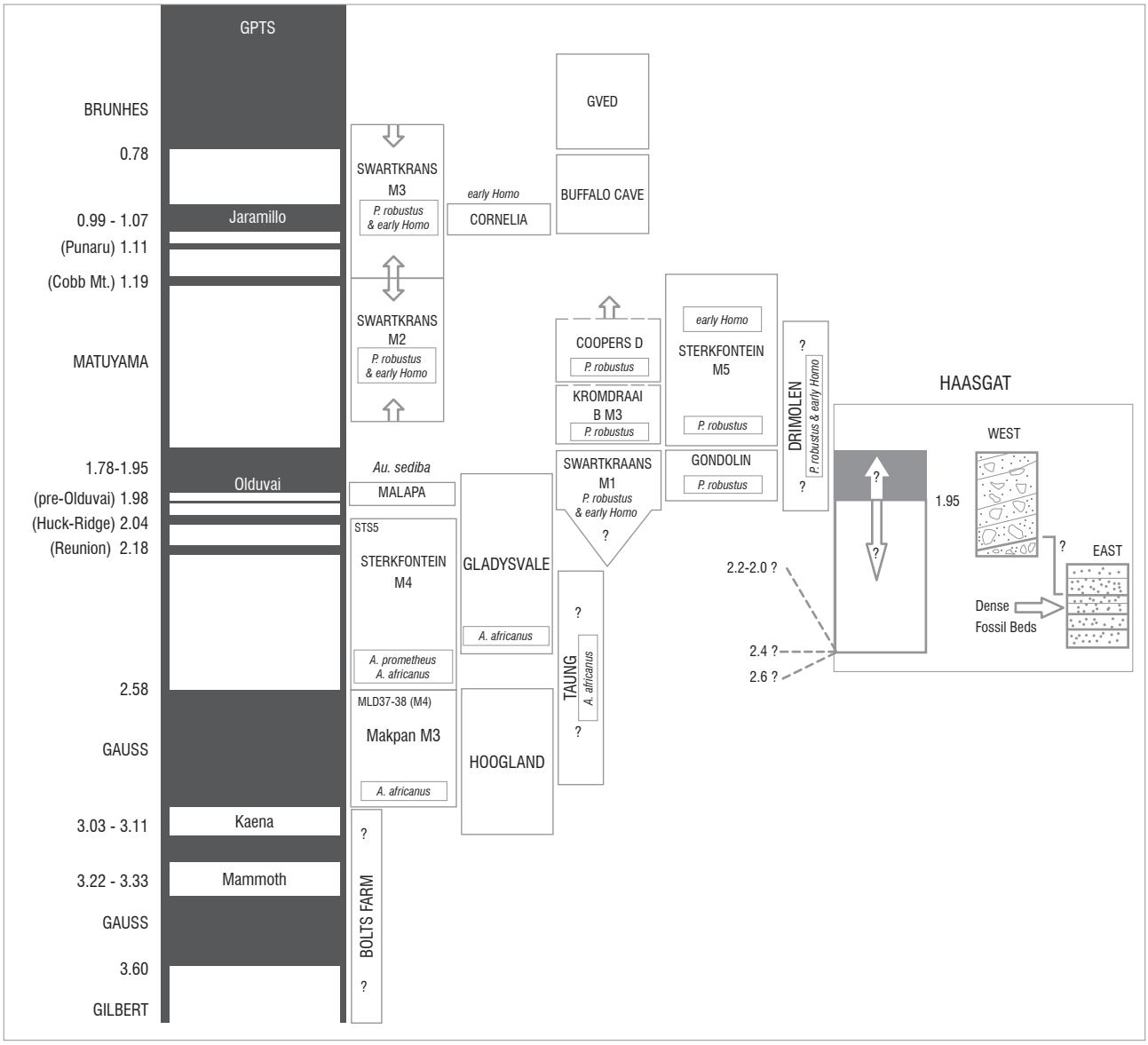

Figure 9: The age of Haasgat on the geomagnetic polarity timescale (GPTS) compared with other hominin and vertebrate fossil bearing sites.

sometime between 2.25 Ma and 1.80 Ma, although more likely between 2.0 Ma and 1.8 Ma[1,7]. Haasgat may also be contemporary with the oldest deposits at the nearby Gladysvale Cave site which are as old as ~2.4 Ma[32] and Member 1 at Kromdraai B, which also records the beginning of the Olduvai SubChron at ~1.95 Ma[56]. While it has been suggested that the ex-situ recovered TM1517 type specimen of *Paranthropus robustus* derives from Kromdraai B Member 1 based on the colour of the adhering matrix[56], all the in-situ hominins from Kromdraai B have come from Member 3, which is estimated to be younger than 1.8 Ma[1]. The Haasgat deposits, with a unique representation of primate and ungulate species, are thus dated to an extremely significant period for human evolution in South Africa with the occurrence of a major turnover in hominin species (*Australopithecus* to *Paranthropus* and *Homo*) and the first occurrence of stone tools that may be related to major climatic and environmental shifts and increased aridity since ~2.2 Ma.[57]

Acknowledgements

This paper and the naming of different portions of the Haasgat site are dedicated to the memory of our recently departed colleagues Andre Keyser (who first worked the Haasgat site), Tim Partridge and Philip Tobias, who all made significant contributions towards understanding the geology and fossil record of South Africa, as well as our colleagues Elizabeth Harmon and Charles Lockwood, whose contributions in the field of hominin anatomy and untimely loss will continue to impact all of us for decades to come. Excavation, survey and fossil sampling and preparation at Haasgat were additionally supported by Lazarus Kgasi of the Plio-Pleistocene Section, Department of Vertebrates, Ditsong National Museum of Natural History in Pretoria under SAHRA permit 80/10/03/010/51 held by Stephany Potze. This project was funded by the Australian Research Council Future Fellowship Grant FT120100399 to A.I.R.H. and a National Science Foundation Grant (NSF BCS 0962564) to J.W.A. The synchrotron analysis was undertaken on the XFM beamline at the Australian Synchrotron (beamtime granted to A.I.R.H. and P.K.). The work was supported by Mimi Hill at the University of Liverpool Geomagnetism Laboratory. We are indebted to Phil Tetley, his family, and the entire Kalkheuvel West community for their support and hospitality during our continued work at Haasgat and SAHRA for issuing us a permit to work at the site. We thank three anonymous reviewers for detailed comments.

Authors' contributions

A.I.R.H. undertook the palaeomagnetic analysis and geological sampling of the site, aided in the latter by J.W.A. J.W.A. and A.D.T.K. undertook the faunal analysis and biochronology of material from the site. A.I.R.H.,

P.K., D.P., D.L.H. and M.D.d.J. undertook the synchrotron XFM work on speleothem from the site. J.W.A., A.I.R.H. and S.P. led the team, decided on site naming and descriptions and recovered the fossils from the site; S.P. holds the permit for the site. S.P. also undertook the acid preparation of the fossil material.

References

1. Herries AIR, Adams JW. Clarifying the context, dating and age range of the Gondolin hominins and *Paranthropus* in South Africa. J Hum Evol. 2013;65:676–681. http://dx.doi.org/10.1016/j.jhevol.2013.06.007
2. Herries AIR, Curnoe D, Adams JW. A multi-disciplinary seriation of early *Homo* and *Paranthropus* bearing palaeocaves in southern Africa. Quat Int. 2009;202:14–28. http://dx.doi.org/10.1016/j.quaint.2008.05.017
3. Herries AIR, Hopley P, Adams JW, Curnoe D, Maslin M. Geochronology and palaeoenvironments of the South African early hominin bearing sites: A reply to 'Wrangham et al., 2009: Shallow-water habitats as sources of fallback foods for hominins'. Am J Phys Anthropol. 2010;143:640–646. http://dx.doi.org/10.1002/ajpa.21389
4. Clarke RJ. Latest information on Sterkfontein's *Australopithecus* skeleton and a new look at *Australopithecus*. S Afr J Sci. 2008;104:443–449.
5. Pickering R, Kramers J. Re-appraisal of the stratigraphy and determination of new U-Pb dates for the Sterkfontein hominin site, South Africa. J Hum Evol. 2010;59:70–86. http://dx.doi.org/10.1016/j.jhevol.2010.09.001
6. Herries AIR, Shaw J. Palaeomagnetic analysis of the Sterkfontein palaeocave deposits: Age implications for the hominin fossils and stone tool industries. J Hum Evol. 2011;60:523–539. http://dx.doi.org/10.1016/j.jhevol.2010.09.001
7. Pickering R, Kramers JD, Hancox PJ, de Ruiter DJ, Woodhead JD. Contemporary flowstone development links early hominin bearing cave deposits in South Africa. Earth Planet Sci Lett. 2011;306:23–32. http://dx.doi.org/10.1016/j.epsl.2011.03.019
8. Berger LR, de Ruiter DJ, Churchill SE, Schmid P, Carlson KJ, Dirks PHGM, et al. *Australopithecus sediba*: A new species of *Homo*-like australopith from South Africa. Science. 2010;328:195–204. http://dx.doi.org/10.1126/science.1184944
9. Dirks PHDM, Kibii JN, Kuhn BF, Steininger C, Churchill SE, Kramers JD, et al. Geological setting and age of *Australopithecus sediba* from southern Africa. Science. 2010;328:205–208. http://dx.doi.org/10.1126/science.1184950
10. Pickering R, Dirks P, Jinnah Z, de Ruiter DJ, Churchill SE, Herries AIR, et al. *Australopithecus sediba* at 1.977 Ma and implications for the origins of the genus *Homo*. Science. 2011;333:1421–1423.
11. Hartstone-Rose A, Kuhn BF, Nalla S, Werdelin L, Berger LR. A new species of fox from the *Australopithecus sediba* type locality, Malapa, South Africa. Trans R Soc S Afr. 2013;68(1):1–9. http://dx.doi.org/10.1080/00359119X.2012.748698
12. Gommery D, Thackeray JF, Sénégas F, Potze S, Kgasi L. The earliest primate (*Parapapio* sp.) from the Cradle of Humankind World Heritage site (Waypoint 160, Bolt's Farm, South Africa). S Afr J Sci. 2008;104(9–10):405–408.
13. Gommery D, Thackeray JF, Sénégas F, Potze S, Kgasi L. Additional fossils of *Parapapio* sp. Waypoint From 160 [Bolt's Farm, South Africa], dated between 4 and 4.5 million years ago. Ann Transv Mus. 2009;46:63–72.
14. Herries AIR, Adams JW, Kuykendall KL, Shaw J. Speleology and magnetobiostratigraphic chronology of the GD 2 locality of the Gondolin hominin-bearing palaeocave deposits, North West Province, South Africa. J Hum Evol. 2006;51:617–631. http://dx.doi.org/10.1016/j.jhevol.2006.07.007
15. Adams JW, Herries AIR, Conroy GC, Kuykendall KL. Taphonomy of a South African cave: Geological and hydrological influences on the GD 1 fossil assemblage at Gondolin, a Plio-Pleistocene palaeocave system in the Northwest Province, South Africa. Quat Sci Rev. 2007;26:2526–2543. http://dx.doi.org/10.1016/j.quascirev.2007.05.006
16. Adams JW. Taphonomy of the Gondolin GD 2 in-situ deposits and its bearing on interpretations of South African Plio-Pleistocene karstic fossil assemblages. J Taphonomy. 2010;8:81–116.
17. Adams JW, Herries AIR, Hemingway J, Kegley A, Kgasi, L, Hopley P, et al. Initial fossil discoveries from Hoogland, a new Pliocene primate-bearing karstic system in Gauteng Province, South Africa. J Hum Evol. 2010;59:685–691. http://dx.doi.org/10.1016/j.jhevol.2010.07.021
18. Brock A, McFadden PL, Partridge TC. Preliminary palacomagnetic results from Makapansgat and Swartkrans. Nature. 1977;266:249–250. http://dx.doi.org/10.1038/266249a0
19. McFadden PL, Brock A, Partridge TC. Palaeomagnetism and the age of the Makapansgat hominid site. Earth Planet Sci Lett. 1979;44:373–382. http://dx.doi.org/10.1016/0012-821X(79)90076-1
20. Herries AIR, Reed K, Kuykendall KL, Latham AG. Speleology and magnetobiostratigraphic chronology of the Buffalo Cave fossil bearing palaeodeposits, Makapansgat, South Africa. Quat Res. 2006;66:233–245. http://dx.doi.org/10.1016/j.yqres.2006.03.006
21. Lacruz RS, Brink JS, Hancox J, Skinner AS, Herries A, Schmidt P, et al. Palaeontology, geological context and palaeoenvironmental implications of a Middle Pleistocene faunal assemblage from the Gladysvale Cave, South Africa. Palaeontol Afr. 2002;38:99–114.
22. Adams JW. A revised listing of fossil mammals from the Haasgat cave system ex situ deposits (HGD), South Africa. Palaeontol Electr. 2012;15(3), Article 29A, 88 pages.
23. Keyser AW, Martini JEJ. Haasgat, a new Plio-Pleistocene fossil locality. Paleoec Aft. 1991;21:119–129.
24. Keyser AW. The palaeontology of Haasgat: A preliminary account. Palaeontol Afr. 1991;28:29–33.
25. McKee J, Keyser AW. Craniodental remains of *Papio angusticeps* from the Haasgat cave site, South Africa. Int J Primatol. 1994;15:823–841. http://dx.doi.org/10.1016/j.jhevol.2010.08.002
26. Plug I, Keyser AW. Haasgat Cave, a Pleistocene site in the central Transvaal: geomorphological, faunal and taphonomic considerations. Ann Trans Mus. 1994;36:139–145.
27. Jablonski N, Frost S. Cercopithecoidea. In: Werdelin L, Sanders W, editors. Cenozoic mammals of Africa. Berkeley: University of California Press; 2010. pp. 393–428. http://dx.doi.org/10.1525/california/9780520257214.003.0023
28. McKee J, Von Mayer A, Kuykendall K. New species of *Cercopithecoides* from Haasgat, North West Province, South Africa. J Hum Evol. 2011;60:83–93.
29. de Ruiter D, Pickering R, Steininger C, Kramers J, Hancox P, Churchill S, et al. New *Australopithecus robustus* fossils and associated U-Pb dates from Cooper's Cave (Gauteng, South Africa). J Hum Evol. 2009;56:497–513. http://dx.doi.org/10.1016/j.jhevol.2009.01.009
30. Geraads D, Raynal J, Eisenmann V. The earliest human occupation of North Africa: A reply to Sahnouni et al. (2002). J Hum Evol. 2004;46:751–761. http://dx.doi.org/10.1016/j.jhevol.2004.01.008
31. Brown FH, Mcdougall I. Geochronology of the Turkana Depression of Northern Kenya and Southern Ethiopia. Evol Anthropol. 2011;20:217–227. http://dx.doi.org/10.1002/evan.20318
32. Herries AIR, Pickering R, Adams JW, Curnoe D, Warr G, Latham AG, et al. A multi-disciplinary perspective on the age of *Australopithecus* in southern Africa. In: Reed KE, Fleagle JG, Leakey R, editors. Paleobiology of *Australopithecus*: Contributions from the Fourth Stony Brook Human Evolution Symposium and Workshop, Diversity in *Australopithecus*: Tracking the First Bipeds. Vertebrate Paleobiology and Paleoanthropology series. Dordrecht: Springer; 2013. p. 21–40.
33. Harris J, White T. Evolution of the Plio-Pleistocene African Suidae. Trans Am Phil Soc. 1979;69:5–128. http://dx.doi.org/10.2307/1006288
34. Brink J, Herries AIR, Moggi-Cecchi J, Gowlett J, Adams JW, Hancox J, et al. First hominine remains from ~1 Ma bone bed at Cornelia-Uitzoek, Free State Province, South Africa. J Hum Evol. 2012;63:527–535. http://dx.doi.org/10.1016/j.jhevol.2012.06.004
35. Adams JW. A methodology for the intraspecific assessment of heterogeneously worn hypsodont teeth using computerized tomography. J Taphonomy. 2005;3:151–612.
36. Kegley ADT, Hemingway J, Adams JW. Odontometric analysis of the reanalyzed and expanded *Cercopithecoides* from the Haasgat fossil assemblage, Cradle of Humankind, South Africa. Am J Phys Anthropol. 2011;S144:183.
37. Latham AG, Herries AIR, Kuykendall K. The formation and sedimentary infilling of the Limeworks Cave, Makapansgat, South Africa. Palaeontol Afr. 2003;39:69–82.

38. Latham AG, Herries A, Quinney P, Sinclair A, Kuykendall K. The Makapansgat australopithecine site from a speleological perspective. In: Pollard AM, editor. Geoarchaeology: Exploration, environments, resources. London: Royal Geological Society, Special Publications. 1999;165:61–77.

39. Latham AG, Herries AIR. The formation and sedimentary infilling of the Cave of Hearths and Historic Cave Complex. Geoarchaeology. 2004;19:323–342. http://dx.doi.org/10.1002/gea.10122

40. Herries AIR. A chronological perspective on the Acheulian and its transition to the Middle Stone Age in southern Africa: the question of the Fauresmith. Int J Evol Biol. 2011;961401, 25 pages.

41. Braun D, Levin N, Stynder D, Herries AIR, Archer W, Forrest F, et al. Mid-Pleistocene hominin occupation of Elandsfontein, Western Cape of South Africa. Quat Sci Rev. 2013;82:145–166. http://dx.doi.org/10.1016/j.quascirev.2013.09.027

42. Vrba ES. The fossil record of African antelopes (Mammalia, Bovidae) in relation to human evolution and paleoclimate. In: Vrba ES, Denton GH, Partridge TC, Burckle LH, editors. Paleoclimate and evolution with emphasis on human origins. New Haven: Yale University Press; 1995. p. 385–424.

43. Herries AIR, Latham AG, Kuykendall K. The use of 'SRT' in palaeomagnetic sampling of the Makapansgat limeworks hominid palaeocave, South Africa. Antiquity. 2001;75:251–252.

44. International Geomagnetic Reference Field: The eleventh generation. International Association of Geomagnetism and Aeronomy, Working Group V-MOD. Participating members: C. C. Finlay, S. Maus, C. D. Beggan, T. N. Bondar, A. Chambodut, T. A. Chernova, A. Chulliat, V. P. Golovkov, B. Hamilton, M. Hamoudi, R. Holme, G. Hulot, W. Kuang, B. Langlais, V. Lesur, F. J. Lowes, H. Luhr, S. Macmillan, M. Mandea, S. McLean, C. Manoj, M. Menvielle, I. Michaelis, N. Olsen, J. Rauberg, M. Rother, T. J. Sabaka, A. Tangborn, L. Toffner-Clausen, E. Thebault, A. W. P. Thomson, I. Wardinski Z. Wei, T. I. Zvereva. Geophys J Int. 2010;183(3):1216–1230. DOI: 10.1111/j.1365-246X.2010.04804.x.

45. Paterson D, De Jonge MD, Howard DL, Lewis W, McKinlay J, Starritt A, et al. The X-ray fluorescence microscopy beamline at the Australian synchrotron. AIP Conf Proc. 2011;1365:219–222. http://dx.doi.org/10.1063/1.3625343

46. Kirkham R, Dunn PA, Kuczewski A, Siddons DP, Dodanwela R, Moorhead G, et al. The Maia spectroscopy detector system: Engineering for integrated pulse capture, low-latency scanning and real-time processing. AIP Conf Proc. 2010;1234:240–243. http://dx.doi.org/10.1063/1.3463181

47. Walden J, Oldfield F, Smith J. Environmental Magnetism: A practical guide. Technical Guide 6. London: Quaternary Research Association; 1999.

48. Dunlop DJ, Özdemir Ö. Rock magnetism: Fundamentals and frontiers. Cambridge: Cambridge University Press; 2001.

49. Zhou H, Greig A, You C-F, Lai Z, Tang J, Guan Y, et al. Arsenic in a speleothem from central China: Stadial-interstadial variations and implications. Environ Sci Technol. 2011;45:1278–1283. http://dx.doi.org/10.1021/es1032103

50. Lascu I, Feinberg JM. Speleothem magnetism. Quat Sci Rev. 2011;30:3306–3320. http://dx.doi.org/10.1016/j.quascirev.2011.08.004

51. Pickering R, Jacobs Z, Herries AIR, Karkanas P, Bar-Matthews M, Woodhead JD, et al. Paleoanthropologically significant South African sea caves dated to 1.1-1.0 million years using a combination of U-Pb, TT-OSL and palaeomagnetism. Quat Sci Rev. 2013;65:39–52. http://dx.doi.org/10.1016/j.quascirev.2012.12.016

52. Latham AG. Paleomagnetism, rock magnetism and U-Th dating of speleothem deposits [PhD thesis]. Ontario: McMaster University; 1981.

53. Latham AG, Ford D. The palaeomagnetism and rock magnetism of cave and karst deposits. In: Aissaoui DM, McNeill DF, Hurley NF, editors. Applications of paleomagnetism to sedimentary geology. Tulsa, OK: Society of Economic Paleontologists and Mineralogists; 1993. p. 150–155.

54. Laj C, Channell JET. Geomagnetic reversals. In: Kono M, editor. Treatise on geophysics: Geomagnetism. Amsterdam: Elsevier; 2007. pp. 373–416. http://dx.doi.org/10.1016/B978-044452748-6.00095-X

55. Gradstein FM, Ogg JG, Schmitz M, Ogg G. The geologic time scale. Boston: Elsevier; 2012.

56. Thackeray JF, Kirschvink JL, Raub TD. Palaeomagnetic analysis of calcified deposits from the Plio-Pleistocene hominid site of Kromdraai, South Africa. S Afr J Sci. 2002;98:537–540.

57. Dupont LM, Donner B, Vidal L, Pérez EM, Wefer G. Linking desert evolution and coastal upwelling: Pliocene climate change in Namibia. Geology. 2005;33:461–464. http://dx.doi.org/10.1130/G21401.1